PHYSICAL REVIEW B **67**, 161308(R) (2003)

Few-electron quantum dot circuit with integrated charge read out

J. M. Elzerman,[1] R. Hanson,[1] J. S. Greidanus,[1] L. H. Willems van Beveren,[1] S. De Franceschi,[1] L. M. K. Vandersypen,[1] S. Tarucha,[2,3] and L. P. Kouwenhoven[1]

[1]*Department of NanoScience and ERATO Mesoscopic Correlation Project, Delft University of Technology, P.O. Box 5046, 2600 GA Delft, The Netherlands*

[2]*NTT Basic Research Laboratories, Atsugi-shi, Kanagawa 243-0129, Japan*

[3]*ERATO Mesoscopic Correlation Project, University of Tokyo, Bunkyo-ku, Tokyo 113-0033, Japan*

(Received 6 February 2003; published 30 April 2003)

We report on the realization of a few-electron double quantum dot defined in a two-dimensional electron gas by means of surface gates on top of a GaAs/AlGaAs heterostructure. Two quantum point contacts are placed in the vicinity of the double quantum dot and serve as charge detectors. These enable determination of the number of conduction electrons on each dot. This number can be reduced to zero, while still allowing transport measurements through the double dot. Microwave radiation is used to pump an electron from one dot to the other by absorption of a single photon. The experiments demonstrate that this quantum dot circuit can serve as a good starting point for a scalable spin-qubit system.

DOI: 10.1103/PhysRevB.67.161308 PACS number(s): 73.23.Hk, 73.63.Kv

The experimental development of a quantum computer is at present at the stage of realizing few-qubit circuits. In the solid state, particular success has been achieved with superconducting devices in which macroscopic quantum states are used to define two-level qubit states (see Ref. 1, and references therein). The opposite alternative would be the use of two-level systems defined by microscopic variables, as realized, for instance, by single electrons confined in semiconductor quantum dots.[2] For the control of one-electron quantum states by electrical voltages, the challenge at the moment is to realize an appropriate quantum dot circuit containing just a single conduction electron.

Few-electron quantum dots have been realized in self-assembled structures[3] and also in small vertical pillars defined by etching.[4] The disadvantage of these types of quantum dots is that they are hard to integrate into circuits with a controllable coupling between the elements, although integration of vertical quantum dot structures is currently being pursued.[5] An alternative candidate is a system of lateral quantum dots defined in a two-dimensional electron gas (2DEG) by surface gates on top of a semiconductor heterostructure.[2] Here, integration of multiple dots is straightforward by simply increasing the number of gate electrodes. In addition, the coupling between the dots can be controlled, since it is set by gate voltages. The challenge is to reduce the number of electrons to one per quantum dot. This has long been impossible, since reducing the electron number decreases at the same time the tunnel coupling, resulting in a current too small to be measured.[6]

In this Rapid Communication, we demonstrate a double quantum dot device containing a voltage-controllable number of electrons down to a single electron. We have integrated it with charge detectors that can read out the charge state of the double quantum dot with a sensitivity better than a single-electron charge. The importance of the present circuit is that it can serve as a fully tunable two-qubit quantum system, following the proposal by Loss and DiVincenzo,[7] which describes an optimal combination of the single-electron charge degree of freedom (for manipulation with electrical voltages) and the spin degree of freedom (to obtain a long coherence time).

Our device, shown in Fig. 1(a), is made from a GaAs/AlGaAs heterostructure, containing a 2DEG 90 nm below the surface with an electron density $n_s = 2.9 \times 10^{11}$ cm^{-2}. This small circuit consists of a double quantum dot and two quantum point contacts (QPC's). The layout is an extension of previously reported single quantum dot devices.[6] The double quantum dot is defined by applying negative voltages to the six gates in the middle of the figure. Gate T in combination with the left (right) gate, L (R), defines the tunnel barrier from the left (right) dot to drain 1 (source 2). Gate T in combination with the middle bottom gate M defines the tunnel barrier between the two dots. The narrow ''plunger'' gate P_L (P_R) on the left (right) is used to change the electrostatic potential of the left (right) dot. The left plunger P_L is connected to a coaxial cable so that we can apply high-frequency signals. In the present experiments, we do not apply dc voltages to P_L. In order to control the number of electrons on the double dot, we use gate L for the left dot and P_R for the right dot. All data shown are taken at zero magnetic field and at a temperature of 10 mK.

We first characterize the individual dots. From standard Coulomb blockade experiments,[2] we find that the energy cost for adding a second electron to a one-electron dot is 3.7 meV. The excitation energy (i.e., the difference between the first excited state and the ground state) is 1.8 meV at zero magnetic field. For a two-electron dot the energy difference between the singlet ground state and the triplet excited state is 1.0 meV at zero magnetic field. Increasing the field (perpendicular to the 2DEG) leads to a transition from a singlet to a triplet ground state at about 1.7 T.

In addition to current flowing through the quantum dot, we can measure the charge on the dot using one of the QPC's.[8,9] We define only the left dot (by grounding gates R and P_R), and use the left QPC as a charge detector. The QPC is formed by applying negative voltages to QPC-L and L. This creates a narrow constriction in the 2DEG, with a conductance G that is quantized when sweeping the gate voltage

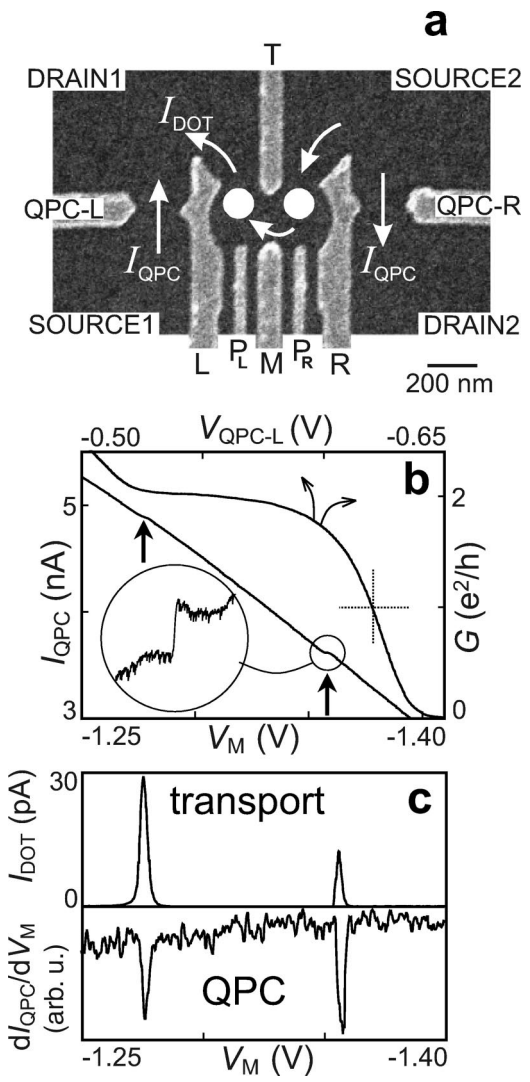

FIG. 1. (a) Scanning electron micrograph of the metallic surface gates. White circles indicate the two quantum dots. White arrows show the possible current paths. A bias voltage V_{DOT} can be applied between source 2 and drain 1, leading to current through the dots I_{DOT}. A bias voltage V_{SD1} (V_{SD2}) between source 1 (source 2) and drain 1 (drain 2), yields a current I_{QPC} through the left (right) QPC. (b) QPC as a charge detector of the left single dot. Upper curve with upper and right axis: conductance G of the left QPC versus the gate voltage V_{QPC-L} showing the last quantized plateau and the transition to complete pinch-off. The dashed line indicates the point of highest charge sensitivity. Lower curve with lower and left axis: current through the left QPC, I_{QPC}, versus left-dot gate voltage V_M. ($V_{SD1}=250\ \mu$V, $V_{DOT}=0$, $V_{SD2}=0$). The steps, indicated by the arrows, correspond to a change in the electron number of the left dot. Encircled inset: the last step (50 pA high), with the linear background subtracted. (c) Upper part: Coulomb peaks measured in transport current through the left dot. Shown is I_{DOT} versus V_M with $V_{DOT}=100\ \mu$V. Lower part: changes in the number of electrons on the left dot, measured with the left QPC. Shown is dI_{QPC}/dV_M versus V_M ($V_{SD1}=250\ \mu$V, $V_{DOT}=0$).

V_{QPC-L}. The plateau at $G=2e^2/h$ and the transition to complete pinch-off (i.e., $G=0$) are shown in Fig. 1(b). At the steepest point, where $G\approx e^2/h$, the QPC conductance has a maximum sensitivity to changes in the electrostatic environment, including changes in the charge of the nearby quantum dot. As can be seen in Fig. 1(b), the QPC current I_{QPC} decreases when we make the left-dot gate voltage V_M more negative. Periodically this changing gate voltage pushes an electron out of the left dot. The associated sudden change in charge increases the electrostatic potential in the QPC, resulting in a steplike structure in I_{QPC} [see expansion in Fig. 1(b), where the linear background is subtracted]. So, even without passing current through the dot, I_{QPC} provides information about the charge on the dot. To enhance the charge sensitivity, we apply a small modulation (0.3 mV at 17.7 Hz) to V_M and use lock-in detection to measure dI_{QPC}/dV_M.[9] Figure 1(c) shows the resulting dips, as well as the corresponding Coulomb peaks measured in the current through the dot. The coincidence of the two signals demonstrates that the QPC indeed functions as a charge detector. From the height of the step in Fig. 1(b) (50 pA, typically 1–2 % of the total current), compared to the noise (5 pA for a measurement time of 100 ms), we can estimate the sensitivity of the charge detector to be about $0.1e$, with e being the single-electron charge. The important advantage of the QPC charge detection is that it provides a signal even when the tunnel barriers of the dot are so opaque that I_{DOT} is too small to measure.[8,9] This allows us to study quantum dots even when they are virtually isolated from the leads.

Next, we study the charge configuration of the double dot, using the QPC on the right as a charge detector. We measure dI_{QPC}/dV_L versus V_L, and repeat this for many values of V_{PR}. The resulting two-dimensional plot is shown in Fig. 2(a). Blue lines signify a negative dip in dI_{QPC}/dV_L, corresponding to a change in the total number of electrons on the double dot. Together these lines form the well-known ''honeycomb diagram.''[10,11] The almost-horizontal lines correspond to a change in the electron number in the left dot, whereas almost-vertical lines indicate a change of one electron in the right dot. In the upper left region the ''horizontal'' lines are not present, even though the QPC can still detect changes in the charge, as demonstrated by the presence of the ''vertical'' lines. We conclude that in this region the *left dot* contains zero electrons. Similarly, a disappearance of the vertical lines occurs in the lower right region, showing that here the *right dot* is empty. In the upper right region, the absence of lines shows that here the *double dot* is completely empty.

We are now able to count the absolute number of electrons. Figure 2(b) shows a zoom in of the few-electron region. Starting from the ''00'' region, we can label all regions in the honeycomb diagram, e.g., the label ''21'' means two electrons in the left dot and one in the right. Besides the blue lines, also short yellow lines are visible, signifying a positive peak in dI_{QPC}/dV_L. These yellow lines correspond to a charge transition between the dots, while the total electron number remains the same. (The positive sign of dI_{QPC}/dV_L can be understood if we note that crossing the yellow lines by making V_L a little more positive means moving an electron from the right to the left dot, which increases I_{QPC}. Therefore the differential quantity dI_{QPC}/dV_L displays a

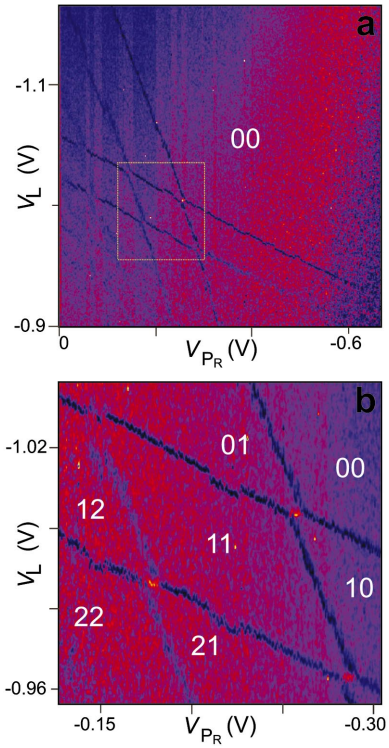

FIG. 2. (Color) (a) Charge stability diagram (''honeycomb'') of the double quantum dot, measured with QPC-R. A modulation (0.3 mV at 17.77 Hz) is applied to gate L, and dI_{QPC}/dV_L is measured with a lock-in amplifier and plotted in color scale versus V_L and V_{PR}. The bias voltages are $V_{SD2}=100$ μV and $V_{DOT}=V_{SD1}=0$. The label ''00'' indicates the region where the double dot is completely empty. (b) Zoom in of (a), showing the honeycomb pattern for the first few electrons in the double dot. The white labels indicate the number of electrons in the left and right dot.

positive peak.) The QPC is thus sufficiently sensitive to detect *interdot* transitions.

In measurements of transport through lateral double quantum dots, the few-electron regime has never been reached.[11] The problem is that the gates, used to deplete the dots, also strongly influence the tunnel barriers. Reducing the electron number would always lead to the Coulomb peaks becoming unmeasurably small, but not necessarily due to an empty double dot. The QPC detectors now permit us to compare charge and transport measurements. Figure 3 shows I_{DOT} versus V_L and V_{PR}, with the dotted lines extracted from the measured charge lines in Fig. 2(b). In the bottom left region the gates are not very negative, hence the tunnel barriers are quite open. Here, the resonant current at the charge transition points is quite high ($\sim$100 pA, dark gray), and also lines due to cotunneling are visible.[11] Towards the top right corner the gate voltages become more negative, thereby closing-off the barriers and reducing the current peaks (lighter gray). The last Coulomb peaks (in the dashed circle) are faintly visible ($\sim$1 pA). They can be increased (up to $\sim$70 pA) by readjusting the barrier gate voltages. Apart from a slight shift, the dotted lines nicely correspond to the regions where a transport current is visible. We are thus able to measure transport through a one-electron double quantum dot.

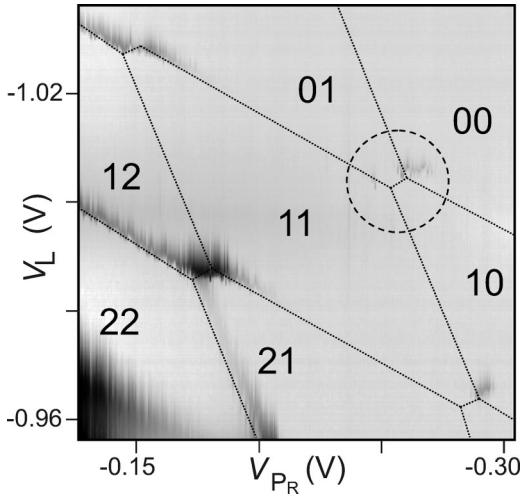

FIG. 3. Transport through the double dot in the same region as Fig. 2(b). Plotted in logarithmic grayscale is I_{DOT} versus V_L and V_{PR}, with $V_{DOT}=100$ μV and $V_{SD1}=V_{SD2}=0$. The dotted lines are extracted from Fig. 2(b). In the light regions current is zero due to Coulomb blockade. Dark gray indicates current, with the darkest regions (in the bottom left corner) corresponding to $\sim$100 pA. Inside the dashed circle, the last Coulomb peaks are visible ($\sim$1 pA). (A smoothly varying background current due to a small leakage from a gate to the 2DEG has been subtracted from all traces.)

The use of gated quantum dots for quantum state manipulation in time requires the ability to modify the potential at high frequencies. We investigate the high-frequency behavior in the region around the last Coulomb peaks (Fig. 4) with a

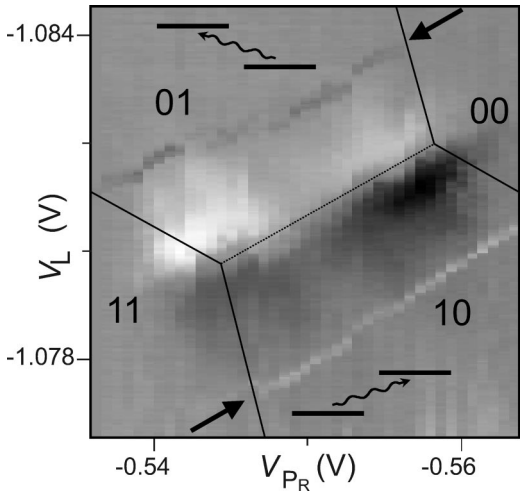

FIG. 4. Photon-assisted transport through the double dot, with zero bias voltage, i.e., $V_{DOT}=V_{SD1}=V_{SD2}=0$. A microwave signal of 50 GHz is applied to P_L. The microwaves pump current I_{DOT} by absorption of photons. This photon-assisted current shows up as two lines, indicated by the two arrows. The white line (bottom) corresponds to pumping from the left to the right reservoir, the dark line (top) corresponds to pumping in the reverse direction. In the middle, around the dotted line, a finite current is induced by an unwanted voltage drop over the dot, due to asymmetric coupling of the ac signal to the two leads (Ref. 11).

50-GHz-microwave signal applied to gate P_L. At the dotted line the 01 and 10 charge states are degenerate in energy, so one electron can tunnel back and forth between the two dots. Away from this line there is an energy difference and only one charge state is stable. However, if the energy difference matches the photon energy, the transition to the other dot is possible by absorption of a single photon. Such photon-assisted tunneling events give rise to the two lines indicated by the arrows. At the lower (higher) line electrons are pumped from the the left (right) dot to the other side, giving rise to a negative (positive) photon-assisted current. We find that the distance between the dotted line and the photon-assisted tunneling lines scales, as expected, linearly with frequency.[11]

The realization of a controllable few-electron quantum dot circuit represents a significant step towards controlling the coherent properties of single electron-spins in quantum dots.[7,12] Integration with the QPC's permits charge read out of closed quantum dots. We note that charge read out only affects the spin state indirectly, via the spin-orbit interaction. The back-action on the spin should therefore be small (until spin-to-charge conversion is initiated), and can be further suppressed by switching on the charge detector only during the readout stage. Present experiments focus on increasing the speed of the charge measurement such that single-shot read out of a single-electron spin could be accomplished.[12,13]

We thank T. Fujisawa, T. Hayashi, Y. Hirayama, C. J. P. M. Harmans, B. van der Enden, and R. Schouten for discussions and help. This work was supported by the Specially Promoted Research, Grant-in-Aid for Scientific Research, from the Ministry of Education, Culture, Sports, Science and Technology in Japan, the DARPA-QUIST program (Grant No. DAAD19-01-1-0659), and the Dutch Organization for Fundamental Research on Matter (FOM).

[1] D. Vion, A. Aassime, A. Cottet, P. Joyez, H. Pothier, C. Urbina, D. Estève, and M.H. Devoret, Science **296**, 886 (2002).

[2] L. P. Kouwenhoven, C. M. Marcus, P. L. McEuen, S. Tarucha, R. M. Westervelt, and N. S. Wingreen, in *Mesoscopic Electron Transport*, Vol. 345 of *NATO Advanced Study Institutes, Series E: Applied Sciences* edited by L. L. Sohn, L. P. Kouwenhoven, and G. Schön (Kluwer Academic, Dordrecht, 1997), pp. 105–214.

[3] P. M. Petroff, A. Lorke, and A. Imamoglu, Phys. Today **54** (5), 46 (2001).

[4] L.P. Kouwenhoven, D.G. Austing, and S. Tarucha, Rep. Prog. Phys. **64**, 701 (2001).

[5] K. Ono, D.G. Austing, Y. Tokura, and S. Tarucha, Science **297**, 1313 (2002).

[6] M. Ciorga, A.S. Sachrajda, P. Hawrylak, C. Gould, P. Zawadzki, S. Jullian, Y. Feng, and Z. Wasilewski, Phys. Rev. B **61**, R16 315 (2000).

[7] D. Loss and D.P. DiVincenzo, Phys. Rev. A **57**, 120 (1998).

[8] M. Field, C.G. Smith, M. Pepper, D.A. Ritchie, J.E.F. Frost, G.A.C. Jones, and D.G. Hasko, Phys. Rev. Lett. **70**, 1311 (1993).

[9] D. Sprinzak, Y. Ji, M. Heiblum, D. Mahalu, and H. Shtrikman, Phys. Rev. Lett. **88**, 176805 (2002).

[10] H. Pothier, P. Lafarge, C. Urbina, D. Estève, and M.H. Devoret, Europhys. Lett. **17**, 249 (1992).

[11] W.G. van der Wiel, S. De Franceschi, J.M. Elzerman, T. Fujisawa, S. Tarucha, and L.P. Kouwenhoven, Rev. Mod. Phys. **75**, 1 (2003).

[12] L.M.K. Vandersypen, R. Hanson, L.H. Willems van Beveren, J.M. Elzerman, J.S. Greidanus, S. De Franceschi, and L.P. Kouwenhoven, quant-ph/0207059 (unpublished).

[13] A. Aassime, G. Johansson, G. Wendin, R.J. Schoelkopf, and P. Delsing, Phys. Rev. Lett. **86**, 3376 (2001).